JOURNAL OF QUATERNARY SCIENCE (2023) **38**(5) 776–789 ISSN 0267-8179. DOI: 10.1002/jqs.3517

JQS Journal of Quaternary Science QRA Quaternary Research Association

Chironomid (Insecta: Chironomidae) community structure response to hydrological changes in the mid-1950s in lake Nam Co, Tibetan Plateau

PAULA ECHEVERRÍA-GALINDO,[1]* SONJA RIGTERINK,[1] JULIETA MASSAFERRO,[2] LISETH PÉREZ,[1] BERND WÜNNEMANN,[3] PHILIPP HOELZMANN,[3] WENGANG KANG,[4] NICOLE BÖRNER,[1] ANJA SCHWARZ,[1] ANDREAS LAUG,[1] PING PENG,[4] JUNBO WANG,[4] LIPING ZHU[4] and ANTJE SCHWALB[1]

[1]Institute of Geosystems and Bioindication, Technische Universität Braunschweig, Braunschweig, Germany

[2]CENAC-National Park "Nahuel Huapi" (PNNH), National Scientific and Technical Research Council of Argentina (CONICET), Bariloche, Argentina

[3]Institute of Geographical Sciences, Physical Geography, Freie Universität Berlin, Berlin, Germany

[4]State Key Laboratory of Tibetan Plateau Earth System, Environment and Resources (TPESER), Institute of Tibetan Plateau Research, Chinese Academy of Sciences, Beijing, PR China

Received 28 May 2021; Revised 19 January 2023; Accepted 29 January 2023

ABSTRACT: The recent rise in air temperatures detected at high altitudes of the Tibetan Plateau has accelerated glacier melt and retreat. Moreover, enhanced monsoonal precipitation has increased runoff and transport of allochthonous material to the lakes. Consequently, water levels are rising, modifying the spatial distribution and composition of local aquatic biota. To infer these environmental and biological changes in recent decades, a 30-cm-long sediment core, representing the past ~160 years, from Nam Co, an endorheic lake, was analyzed for subfossil chironomid assemblages and sediment geochemistry. In total, 25 chironomid morphotypes were identified. Nineteen were considered as non-rare taxa (abundances ≥2%) and six as rare taxa (abundances <2%). Since 1956 CE, higher chironomid richness (S = 19) is evident compared to the previous 100 years. The simultaneous decrease in the abundance of profundal *Micropsectra radialis*-type and increase of both *Chironomus* and *Procladius*, taxa adapted to more eurytopic and slightly warmer water bodies, indicate increasing water temperatures and intensified primary productivity. The dominance of littoral chironomid assemblages reflects increasing lake water levels, flooded shorelines and expansion of littoral areas driven by increased precipitation and glacial meltwater input both resulting from the increase in air temperatures. This scenario is confirmed by increases in total nitrogen and Zr/Rb ratios, indicating higher productivity and coarser grain size as a consequence of increased runoff via the Niya Qu. These hydrological changes have resulted in a positive water balance that can be linked to an increase in moisture supply from the Indian summer monsoon and glacier melt, reflecting increasing temperatures and precipitation since 1956 CE, ultimately driven by anthropogenic warming.

KEYWORDS: chironomid; Indian summer monsoon; Nam Co; Niya Qu; nutrients; runoff; water level

Introduction

High-altitude lakes play an important role in the study of global climate variability and ecosystem responses because of their high sensitivity to global changes as well as their remote and undisturbed locations (Chang et al., 2017; Wu et al., 2020). The Tibetan Plateau (TP; average altitude >4000 m above sea level) is one of the regions of the world most affected by global warming starting in the 19th century (Anslan et al., 2020). A significant warming trend has been observed on the TP since the 1950s, with a range from 0.16 to 0.67 °C per decade, which is faster than that over the Northern Hemisphere and the northern midlatitudes (Zhou and Zhang, 2021), and overall twice as fast as the global average (Anslan et al., 2020). As a consequence, nearly all TP glaciers have retreated, causing a 5.5% increase in river runoff from the Plateau (Yao et al., 2007) and increased runoff and transport of allochthonous material into TP lakes (Luoto, 2010; Zhang et al., 2011; Lei et al., 2013; Jiang et al., 2017).

*Correspondence: Paula Echeverría-Galindo, as above.
Email: p.echeverria-galindo@tu-braunschweig.de

Since the 1970s, satellite images have shown glacier shrinkage in the Nyainqêntanglha mountain range at a rate of 0.3–0.5% a^{-1}. As a result of glacier melting, the lake surface of Nam Co has expanded from ~1930 km^2 to ~2018 km^2 at a rate of 2.1 km^2 a^{-1} (0.1% a^{-1}) and lake level has risen at a rate of 0.3 m a^{-1} until about 2009, and at lower rates since then (Anslan et al., 2020). In addition to glacier melt, meteorological station data on the TP (Yang et al., 2011; Lei et al., 2014; Yang K. et al., 2014) as well as climate models (Su et al., 2013) show that precipitation has increased over the last 40 years (Sun et al., 2020; Yao et al., 2022). Precipitation regimens in the Nam Co region depend on the Asian summer monsoon (ASM) system and the Westerlies (Morrill, 2004; Bolch et al., 2010); the ASM consists of the Indian summer monsoon (ISM), also known as South Asian summer monsoon, and the East Asian summer monsoon (EASM) (Yao et al., 2013). Studies from the Naqu region, in which Nam Co is located, have reported an increase in annual precipitation of 15 mm per decade from 1970 to 2010 CE (Fang et al., 2016), causing an increase in lake water levels (Ma et al., 2016; Jiang et al., 2017; Yang et al., 2017; Zhang et al., 2021; Yao et al., 2022). Thus, the combination of both increasing precipitation and increasing meltwater supply has caused more surface runoff and transport of material into the lake via higher fluvial transport (Schütt et al., 2010). Elevated nutrient supply resulting from increased runoff has consequently led to increased nutrient supply, further augmented by more intensive livestock grazing in the area. This has resulted in rising total nitrogen (TN) values (0.10–0.37%) in Nam Co sediments during the last 250 years (Wang et al., 2012; Kasper et al., 2013). Previous studies have shown that highest concentrations of total organic carbon (TOC), TN and n-alkanes in surface sediments from the small eastern basin of Nam Co reflect high organic contents and nutritional levels, as well as a suitable environment for aquatic plant growth supported by riverine input of terrigenous detritus and nutrients (Wang et al., 2012). High nutrient concentrations in the deep lake basin, especially those associated with terrestrial inputs, indicate that nutrient enrichment occurs via deposition in the center of the lake, where the anaerobic environment preserves sedimentary organic matter (Wang et al., 2012). Therefore, even during winter, when cold conditions limit surface water input, and parts of the lake are covered by ice, preventing physical mixing, the dissolved organic matter (DOM) content is still sufficient to support biological and chemical processes in the lake (Spencer et al., 2014). As mentioned by Rue et al. (2019), in winter, phytoplankton activity produces oxygen in the upper water column, the ice cover prevents water mixing, causing oxygen reduction through detritus and sediment decomposition at the lake bottom (Mathias and Barica, 1980; Golosov et al., 2006). The temperature dynamics of a frozen lake are essential in determining the formation and persistence of anoxic conditions (Golosov et al., 2006). Factors affecting the heat storage capacity of sediments can modulate the velocity and duration of anoxic conditions in the lake, such as the presence of a stable stratification in the water column, obstructing heat distribution and establishing physio-chemical gradients responsible for regulating solute movement (Bengtsson, 1996; Golosov et al., 2006).

These considerable changes in the lake ecosystem also alter the spatial distribution and composition of inhabiting species (Walther et al., 2010). The littoral zones of high-altitude and stratified lakes, such as Nam Co, offer heterogeneous habitats for a wide range of taxa. High oxygen availability and light intensity have been shown to influence the distribution of biological assemblages (Raposeiro et al., 2018; Wu et al., 2020). The position and extent of littoral habitats depend on water level and the morphological characteristics of the lake shore (Brodersen and Lindegaard, 1997), but also are a result of water temperature and input of organic material (Nazarova et al., 2015, 2017). In contrast to the profundal zones of lakes, littoral areas are characterized by a higher abundance of aquatic plants and high nutrient contents (Wu et al., 2020), providing shelter and high food availability for a great variety of organisms. Chironomids (Diptera: Chironomidae) are the most abundant insect family in freshwater habitats (Brooks et al., 2007). Their larval head capsules are chitinous and preserve well in lake sediments (Walker, 1987). The larvae of chironomids are affected directly (growth and survival) and indirectly (habitat and food) by many different temperature-dependent variables such as productivity, oxygen availability and ice-cover duration (Eggermont and Heiri, 2012), which are also influenced by the availability of organic matter and nutrients. A diverse chironomid community depends on the macrophyte community and sediment substrates (Langdon et al., 2010). Due to their high sensitivity to environmental changes, chironomids are considered as excellent tools in paleoenvironmental reconstructions (Battarbee, 2000; Brooks et al., 2007). They are used to infer, for example, past climate changes, trophic state, salinity and water level (Brooks, 2006).

Only a few studies have used chironomids in the high-mountain regions of the TP (Plank, 2010; Chang et al., 2017; Zhang et al., 2017; Laug et al., 2020). Most of these studies focused on modern training sets to develop transfer functions with the goal to infer mean summer temperatures. Only one study has addressed hydrological changes in a small, shallow lake (Rigterink et al., 2022). None of these studies, however, has considered the consequences that hydrological changes may have had for chironomid communities and lake productivity on the south-central TP in recent years. Therefore, the focus of this study was to investigate the response of chironomid assemblages to habitat changes in Nam Co linked to climatic and environmental change in recent decades.

Study site

Nam Co (30°40′N, 90°30′ E) is located on the south-central TP (Wang et al., 2019) (Fig. 1) a region affected by semi-arid to sub-humid climates (Wang et al., 2011). The climate at Nam Co is primarily influenced by the ISM and the Westerlies (Morrill, 2004; Bolch et al., 2010). Mean annual air temperature measured at the Nam Co Monitoring and Research Station for Multisphere Interactions (NAMORS) was −0.6 °C (from 2006 to 2017, Anslan et al., 2020), while the mean temperature of the coldest and warmest months were −9.6 and 7.0 °C, respectively (Anslan et al., 2020). Annual precipitation ranged between 291 and 568 mm (Anslan et al., 2020). Most precipitation occurs during the ISM season between May and September (Keil et al., 2010; Wrozyna et al., 2010). Precipitation rates are spatially highly variable due to the >7000-m-high Nyainqêntanglha mountain range which represents the southern border of the Nam Co catchment (Bolch et al., 2010). In the Nam Co catchment the glacier area decreased by 6.1 ± 3% between 1976 and 2001 (Bolch et al., 2010). During summer, up to 60 temporary rivers drain into the lake, most of them at the western and southern shores (Kai et al., 2020). The Niya Qu (Qu means river), originating in a non-glaciated catchment (Zhou et al., 2013), feeds the lake throughout the year and enters at the eastern part of the Nam Co basin. In contrast, the majority of the temporary rivers originate from the north-western slopes of the Nyainqêntanglha mountain range, discharging glacial meltwater into the lake (Mügler et al., 2010). Nam Co is endorheic and therefore water loss occurs mainly through evaporation (Mügler et al., 2010; Doberschütz et al., 2014).

Nam Co is a large dimictic lake (surface area ~2026 km^2) located at 4730 m above sea level (a.s.l.). The maximum water depth is ~99 m (Kai et al., 2020). Lake water is alkaline (pH 7.8–9.5), salinity ranges between 0.9 and 2.1 $g\,L^{-1}$ (Keil et al., 2010; Kasper et al., 2013), and electric conductivity between 1851 and 1920 $\mu S\ cm^{-1}$ with a dominance of Na^+ and HCO_3^- (Keil et al., 2010; Huang et al., 2017). The lake is stratified from early June to early November with a thermocline at ~20-m water depth (Kasper et al., 2013; Huang et al., 2017; Wang et al., 2019), and surface water temperatures reaching up to 12 °C. During winter, the lake is ice-covered from January or February to April or May (Huang et al., 2017), and the entire water column mixes in the central part. Interannual variation in snow and ice-cover leads to drastic changes in winter heating of the water column. Thus, thermal fluxes control the seasonal evolution of water column stratification (Wang et al., 2020). Like other high-altitude lakes on the TP, Nam Co is oligotrophic and characterized by low in-lake productivity (TOC of 1.07% and TN of 0.19%; Wang et al., 2012). In July 2018, surface water temperature was

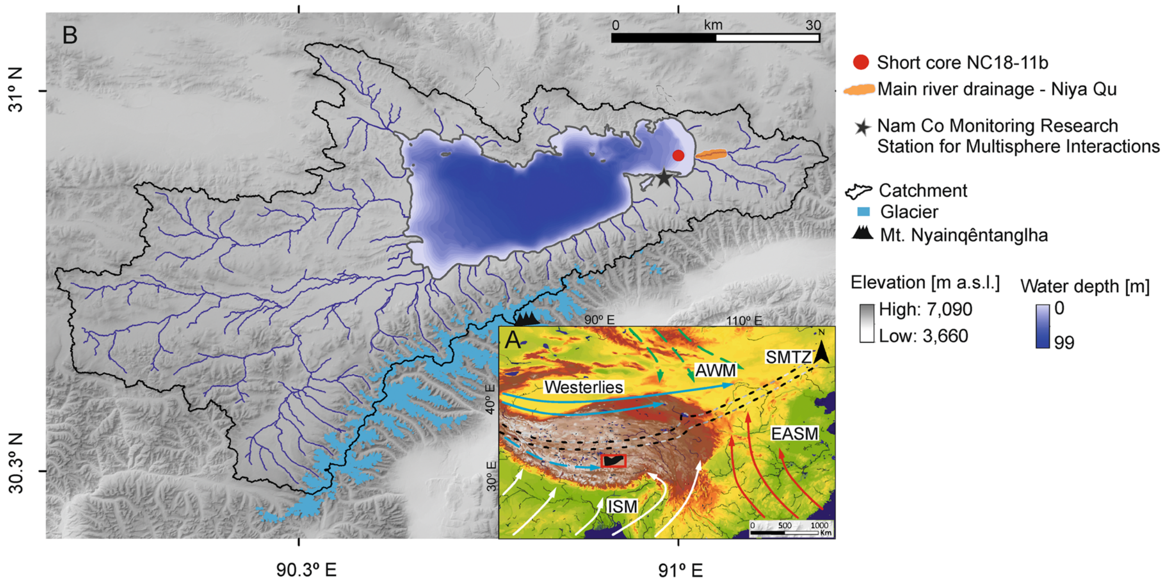

Figure 1. Map showing (A) atmospheric systems influencing the Tibetan Plateau. Continuous arrows indicate systems active in summer: Indian summer monsoon – ISM (white, left-down), East Asian summer monsoon – EASM (red, right) and the Westerlies (blue, left-top). Dashed lines indicate systems active in winter: Asian Winter Monsoon – AWM (green, top) and southern parts of the Westerlies (blue, left-down). The black dotted lines denote the summer monsoon Transition Zone – SMTZ (modified from Anslan et al., 2020). (B) Location of the core (NC18-11b, red dot) and the Nam Co Monitoring and Research Station for Multisphere Interactions (NAMORS) (black star) in the Nam Co catchment. [Color figure can be viewed at wileyonlinelibrary.com]

9.6 °C, conductivity 1305 µS cm^{-1}, pH 10.1, alkalinity 18.4 mmol L^{-1} and transparency (Secchi disk) 9 m.

Methods

Field work

The 30-cm sediment core NC18-11b was retrieved from the north-eastern basin of Nam Co (30°41′51.43″N, 90°58′46.02″ E) in July 2018, using an UWITEC piston corer. Water depth was 27 m at the core location. The closest distance to the shore was 6.3 km, where the Niya Qu enters Nam Co (Fig. 1).

Laboratory work

Lithological description

The sediment core was split lengthwise. Each section was cleaned with a glass slide and distilled water, and photographed using a Canon camera. Core sedimentology and color were described by visual inspection of the cleaned sediment surface using the Munsell Color Chart (Munsell 2010).

Chronology

Dried sediment samples from the uppermost 20 cm were analyzed each 1 cm for ^{210}Pb, ^{226}Ra and ^{137}Cs by direct gamma assay at the Environmental Radiometric Facility, University College London, using an ORTEC HPGe GWL series well-type coaxial low background intrinsic germanium detector. ^{210}Pb was determined via its gamma emissions at 46.5 keV, and ^{226}Ra by the 295- and 352-keV gamma rays emitted by its daughter isotope ^{214}Pb, following 3 weeks of storage in sealed containers to allow for radioactive equilibration. ^{137}Cs was measured by its emission at 662 and 59.5 keV (Appleby et al., 1986). The absolute efficiencies of the detector were determined using calibrated sources and sediment samples of known activity. Corrections were made for the effect of self-absorption of low-energy gamma rays within the sample (Appleby et al, 1986). Four bulk sediment samples were used for radiocarbon dating at Beta Analytic Radiocarbon Dating (FL, USA). Radiocarbon dates were calibrated using IntCal 20 Northern Hemisphere calibration (Reimer et al., 2020). The age–depth model was built using Calib 8.1.0 (Reimer et al., 2020). All ages are expressed in calendar years (CE hereafter).

Sediment–geochemical analysis

Sub-samples were collected at 2-cm intervals, oven dried at 50 °C for 24 h and ground to a fine powder. Elemental analyses, total carbon (TC), total inorganic carbon (TIC) and TN were analyzed at the Institute of Geographical Sciences at the Freie Universität Berlin, Germany. For elemental analyses, dry powdered samples were placed into plastic cups, sealed with a mylar foil (0.4 µm) and analyzed with an Analyticon NITON XL3t portable energy-dispersive X-ray fluorescence spectrometer (P-ED XRF). Only selected elements that had minimum values four times larger than their first measurement uncertainty were considered (Al, Ca, P, Rb, Si, Sr, Ti, Zr). All element ratios were calculated as molar element ratios. Si, Rb, Ti and Zr are allochthonous elements and indicative of minerogenic input to the lake (Kylander et al., 2011). Zr/Rb is used to acquire information on grain size changes with lower values representing fine-grained material and higher values representing coarse-grained material (Dypvik and Harris 2001; Chen et al. 2006). Ca and Sr are regarded as authigenic elements and are related to the in-lake precipitation of carbonates. Phosphorus (P) is a potentially limiting nutrient that sustains primary productivity and has been recognized as a key factor responsible for eutrophication (Wang and Morrison, 2014). When P is corrected for grain size [P*(Zr/Rb)], high values indicate more terrestrial input. TC and TN were determined with a LECO TruSpec CHN-analyzer by combustion of 100 mg of dried sample in an O_2-stream at 950 °C and CO_2-detection by infrared spectroscopy (TC) and thermal conductivity measurement (TN). A Wösthoff Carmhograph C-16 was used to determine TIC after evolving CO_2 from 100 mg of the dried sample by adding 42.5 mg H_3PO_4. The evolved CO_2 produced a change of conductivity in NaOH, representative of the TIC content of the sample. TOC was calculated by subtracting TIC from TC. TOC and TN were used to calculate the C/N element molar ratios for those samples that showed TOC values >0.7%. We examined qualitative and semi-quantitative mineralogical compounds by X-ray powder diffraction with a RIGAKU Miniflex600 diffractometer at 15 mA/40 kV (Cu kα) from 3° to 80° (2θ) with a goniometer step velocity of 0.02° steps and 0.5° min^{-1}. We used the software X-Pert HighScore Version 1.0b by PHILIPS Analytical B.V. for semi-quantitative identification of the mineral composition. Within this program, outliers were corrected, the $k\alpha_2$-peaks were eliminated, and the 2θ angles were calibrated to the quartz peak with an intensity of 100 main peak ($d = 3.34$ Å). Powder Diffraction Files (PDFs) of the ICDD (International Centre for Diffraction Data) were used to identify the peaks. The XRD results are expressed in counts per second (cps) which reflects semi-quantitatively the proportion of the minerals.

Chironomid analysis

Sub-samples were collected at 0.5-cm intervals throughout the core. These samples were prepared with potassium hydroxide solution (10%) and heated for 20 min at 80–90 °C (Walker, 1987). The deflocculated sediment was passed through a nylon mesh (100 µm). Head capsules (HCs) were hand-picked with a stereo-microscope at 32× and 16× magnification. To get a statistically significant number of taxa, the minimum HC count was set to 45 per dry sample (Engels et al., 2020). Only non-rare taxa (abundances ≥2%) were used in the statistical analysis. Rare taxa (abundances < 2%) are shown in Fig. S2. Chironomidae identification followed Brooks et al. (2007), Bitušík and Hamerlík (2014), and Laug et al. (2019). Morphotypes were photographed using a Zeiss Axio ImagerA2 microscope with an AxioCam HRc camera.

Statistical analysis

Percentages of chironomid relative abundances were plotted using C2 software (Juggins, 2007). Biological and non-biological data were square-root transformed and standardized, respectively. A constrained hierarchical cluster analysis (Grimm, 1987) was performed using a Bray–Curtis distance and CONISS linkage method to define chironomid stratigraphic zones. The statistical significance of the clusters was assessed using a broken-stick model (Bennett, 1996). For diversity analysis, rarefaction was calculated (Engels et al., 2020). Non-metric multidimensional scaling (NMDS), using Bray–Curtis distances, was performed to detect the environmental variables that affect the Chironomidae ordination, and to detect the changes in assemblage composition (Kenkel and Orlóci, 1986). Selected environmental variables were chosen based on the known chironomid distribution in modern environmental gradients (*prior* knowledge) and variables with the highest variance percentages obtained by NMDS analysis. All analyses were performed using R with the packages *Rioja* and *Vegan* (Version 1.1.456; RStudio, Inc.).

Results

Chronology

The chronology of the core is based on radionuclide dating (^{137}Cs/^{210}Pb). Four additional radiocarbon ages (Table S1) were excluded due to high and variable reservoir effects. The fixed age in the ^{137}Cs/^{210}Pb model was based on the zero value for Cs at 13 cm depth (1950 CE, Hua et al., 2013). The age model was based on the constant rate of supply (CRS model, Abril, 2004) and provides sediment accumulation rates (SARs) of 0.18–0.27 cm a^{-1}. SARs were calculated based on the tie points in the ^{137}Cs record at 3.25 cm (1987 CE), 9.75 cm (1963 CE) and 13.25 cm depth (1950 CE) and linearly extrapolated to 30-cm depth (Fig. 2). Hence, the record covers the period from 2018 CE back to 1861 CE. The high ^{210}Pb and ^{137}Cs values at 3 cm sediment depth may represent the Chernobyl nuclear disaster in 1986 CE. Due to the possible migration of ^{210}Pb through the sediment that may have produced unreliable timing according to the equations of Appleby and Oldfield (1978) and Appleby (2008), we prefer to rely on the ^{137}Cs data.

Based on the ^{137}Cs and ^{210}Pb age models, the ^{14}C ages may suffer from variable reservoir effects caused by the incorporation of old ^{14}C. We calculated reservoir errors (REs) of 1360, 4755 and 4830 years when we applied the age–depth models

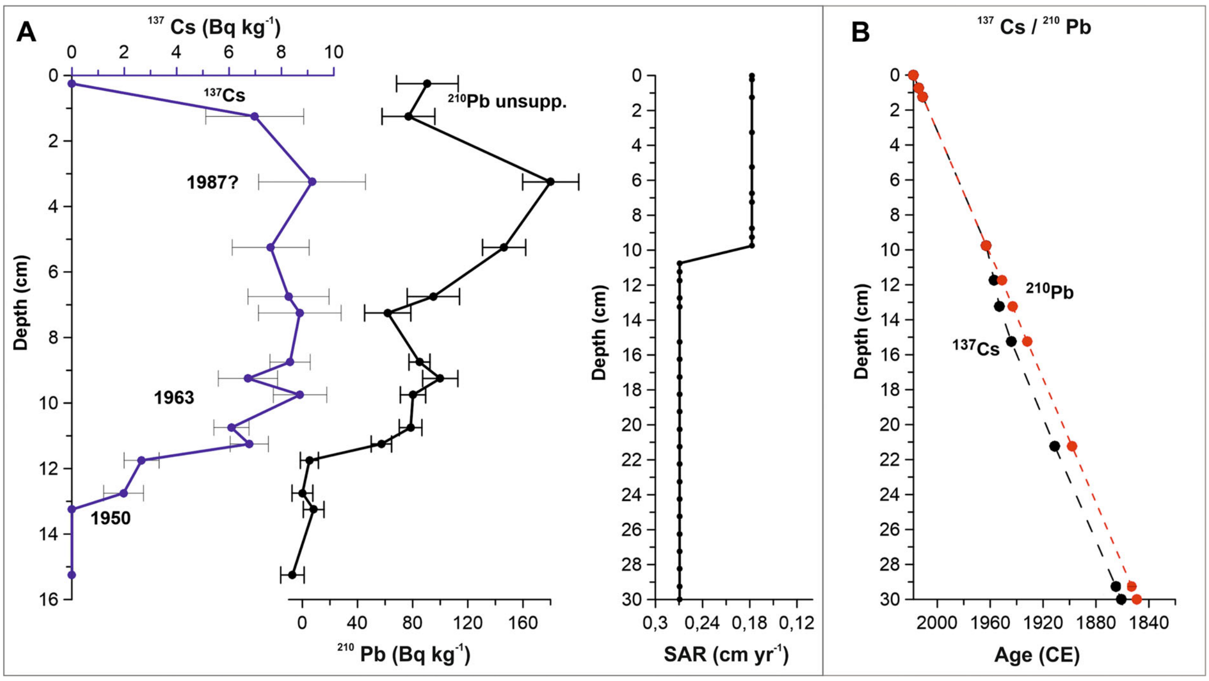

Figure 2. Age–depth correlation for Nam Co sediment core NC18-11b. (A) Measurements of ^{137}Cs and ^{210}Pb for the upper 15 cm and sediment accumulation rates (SAR). (B) Age model comparison using ^{137}Cs (black) and ^{210}Pb (red). [Color figure can be viewed at wileyonlinelibrary.com]

obtained by ^{137}Cs and ^{210}Pb dating. A similar average RE of 1230 years of surface sediments of Nam Co was reported by, for example, Zhu et al. (2008), supporting our findings. Such variable and high REs are very common in lake systems of the TP and adjacent regions, where old carbon is introduced by rivers from the catchment, as an effect of the prolonged exchange of dissolved inorganic carbon in lake water with atmospheric CO_2 and the increased influence of currents and groundwater free or poor in ^{14}C due to the dissolution of carbonaceous basement rocks (e.g. Mischke et al., 2013; Lockot et al., 2015; Hua et al., 2013; Wünnemann et al., 2018). Along the core, a hiatus is discarded because no sharp changes in the sediment composition (Fig. S1) that could indicate a break in sedimentation were detected.

Core description – sedimentology

The water content in core NC18-11b varies only slightly within the range 49.0–58.4%.The lower part of the sediment core (30–12 cm, representing 1861–1956 CE) is characterized by light-yellow (Hue 7.5 Y 7/3) clayish silt, containing shell fragments and a few plant remains, especially between 30 and 26.5 cm (Fig. 3). All element relative values are low, except for Ti/Al ratios, which are moderately high. The only important change in trends is observed between 28 and 24 cm (1872–1895 CE), where dolomite, quartz and clay minerals decrease, while C/N and silicates (orthoclase, albite and epidote) increase. A slight increase of P*(Zr/Rb) is also observed when low-Mg calcite (<4 mol% $MgCO_3$) contents decrease. In the upper part of the core, between 12 and 0 cm (1956–2018 CE), silty-sandy sediments of light gray color (Hue 2.5 Y 7/2) and a more organic-rich substrate with plant remains characterizes the record. All elements change trends at 10.5 cm (1962 CE). There is a concomitant increase in Sr/Ca, Zr/Rb and Ti/Al, whereas low-Mg calcite decreases in the upper 12 cm. P*(Zr/Rb) is higher in the uppermost part, reaching a maximum value of 3171 ppm at 1 cm. TOC values and C/N ratios are slightly lower (1.10 and 5.20%, respectively) than at the bottom (1.44 and 8.06%, respectively) of the core, while TC values (7.10–8.60%, mean 7.82%) are higher. From 10.5 cm towards the top of the core TN increases. The mineralogical composition of the sediments consists of carbonates [low-Mg calcite, monohydrocalcite (MHC) and dolomite], silicates (orthoclase, albite and epidote), quartz, feldspars, clay minerals (halloysite, chlorite) and pyrite. Low-Mg calcite is the main mineralogical component of the entire core but decreases from 12 cm to the top. An opposite trend is observed for dolomite and MHC that show highest contents when low-Mg calcite decreases. The increase in dolomite and MHC is paralleled by increased intensities of quartz and silicates, whereas clay minerals show varying contents that are generally lower in the upper 12 cm. Pyrite is present along the entire core, except for between 10 and 8 cm. In the upper 2 cm (since 2006 CE), all element and mineral trends decrease considerably, except for Sr/Ca and P*(Zr/Rb) that increase, and low-Mg calcite that maintains low values.

Chironomid assemblages

A total of 3675 HCs belonging to 25 chironomid morphotypes (Fig. 4) were identified down to the genus or morphotype level. From the total, 19 morphotypes were considered as non-rare taxa (relative abundances = 2–80%) and six morphotypes as rare taxa (abundances <2%). The assemblages are composed of four subfamilies with Orthocladiinae being the most abundant (17 morphotypes), followed by Chironominae (six morphotypes), Prodiamesinae and Tanypodinae (one morphotype each) (Table S2). A total of 138 HCs were assigned to Tanytarsini (tribe Tanytarsini, subfamily Chironominae) and 10 head capsules to Orthocladiinae, subfamily Orthocladiinae. A mean value of 61 HCs per sample were counted (range: 37–97). The CONISS and broken-stick analysis (Fig. S3) allowed us to recognize two zones along the chironomid profile (Fig. 5, 6).

Zone I (30–12 cm = 1861–1956 CE): *Micropsectra – Paratanytarsus* assemblage. This zone is dominated by *Micropsectra radialis*-type (mean abundance 73%) followed by *Paratanytarsus austriacus*-type (19%) (Figs. 4 and 6). *Chironomus* (0–12%), *Acricotopus* indet. morphotype *incurvatus* (0–5%) and *Procladius* (0–5%) were also present in minor abundances. *Acricotopus* type K, *Tanytarsus lugens*-type, *Monodiamesa*, *Orthocladius rivulorum*-type, *Tanytarsus cf. gracilentus*-type, *Cricotopus bicinctus*-type, *C. shilovae*-type, *C. intersectus*-type and *Paracladius* occurred

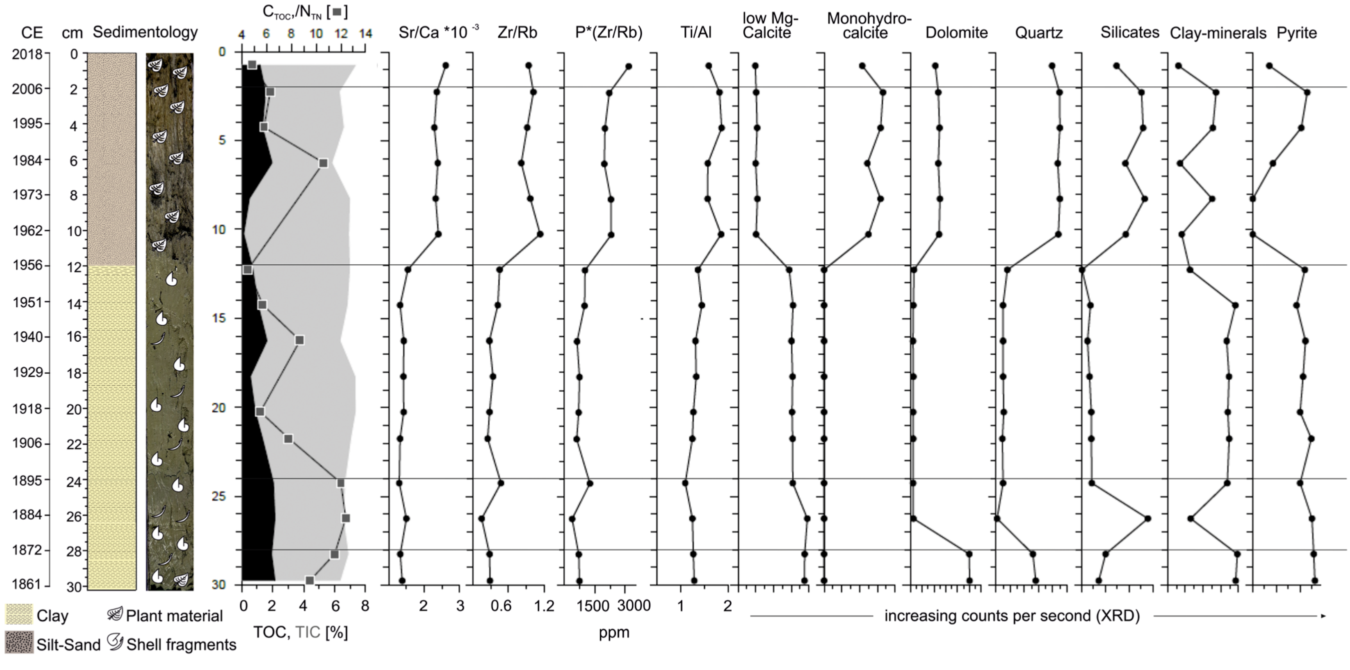

Figure 3. Sediment description and geochemical data for the 30-cm-long core NC18-11b covering the last approximately 160 years. [Color figure can be viewed at wileyonlinelibrary.com]

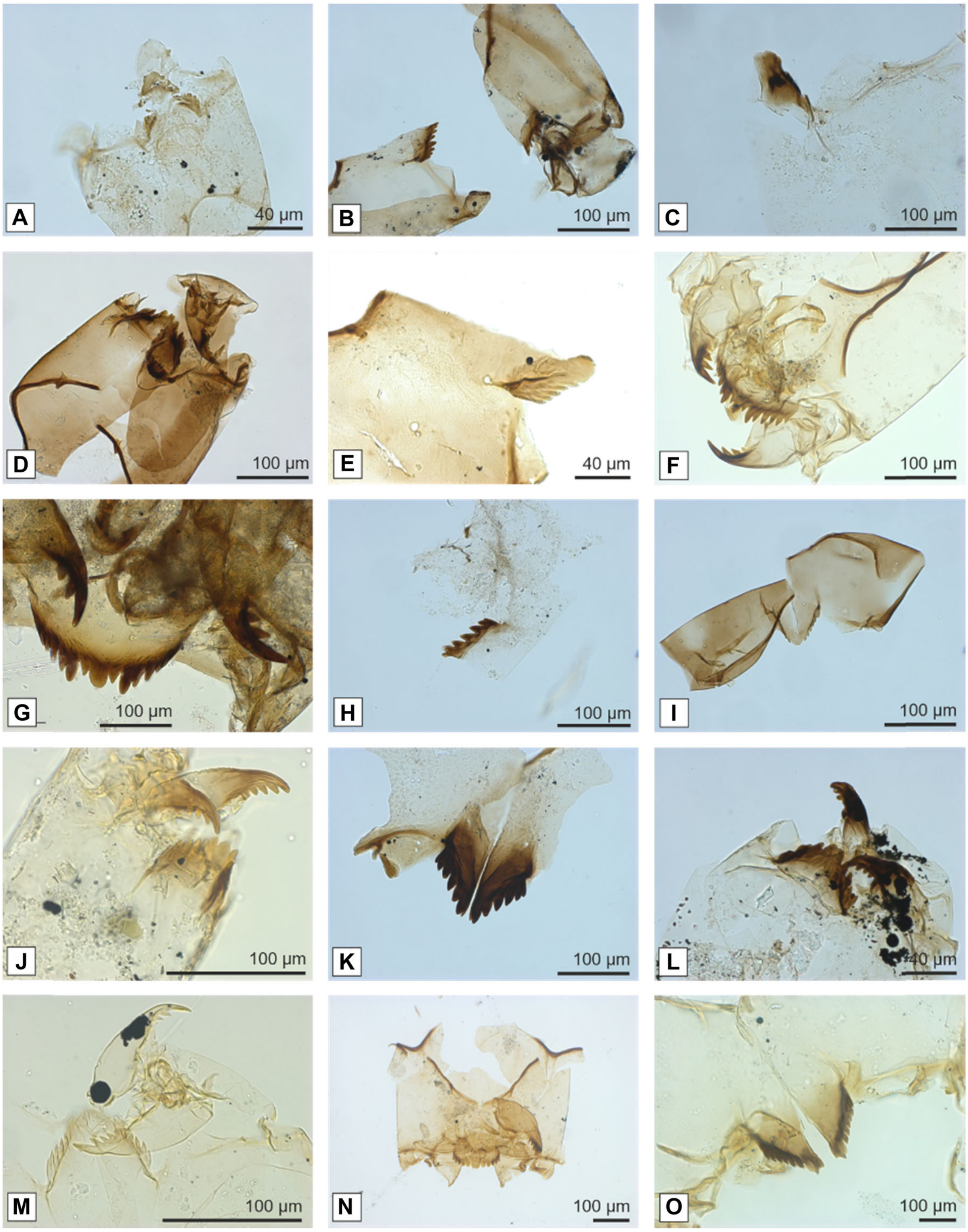

Figure 4. Light micrographs of chironomid morphotypes. [Color figure can be viewed at wileyonlinelibrary.com]

sporadically. In general, two peaks of higher abundances of HCs were detected at 23 cm (133 HC g^{-1}) and 19 cm (196 HC g^{-1}) (Fig. 6).

Zone II (12–0 cm, representing 1956–2018 CE): *Chironomus – Procladius* assemblage. The abundances of *Micropsectra radialis*-type decreased, while *Chironomus* sp. increased in the upper 12 cm. Most of the types that occurred sporadically in Zone I increased in this zone (Fig. 6). In addition, four types (i.e. *Acricotopus lucens*-type, *Pseudosmittia* type B, *Orthocladius* type S and *Psectrocladius sordidellus*-type, Fig. 4) were detected for the first time with abundances of >5%.

Diversity analysis

The comparison between the rarefied (calculated) number of taxa and the observed number of taxa shows a linear trend for Zone I, while the values diverge for Zone II (Fig. 5A). A lower number of taxa were identified for Zone I than for Zone II. However, the curves for the rarefied taxa reach the asymptote for Zone I (Fig. 5B), indicating that the maximum number of taxa in the sediment core was detected. Based on the rarefied number of morphotypes, the diversity in this zone fluctuates between four and nine (mean value 5.8). In Zone II, the diversity is higher (mean value 10.9), with a maximum of 15

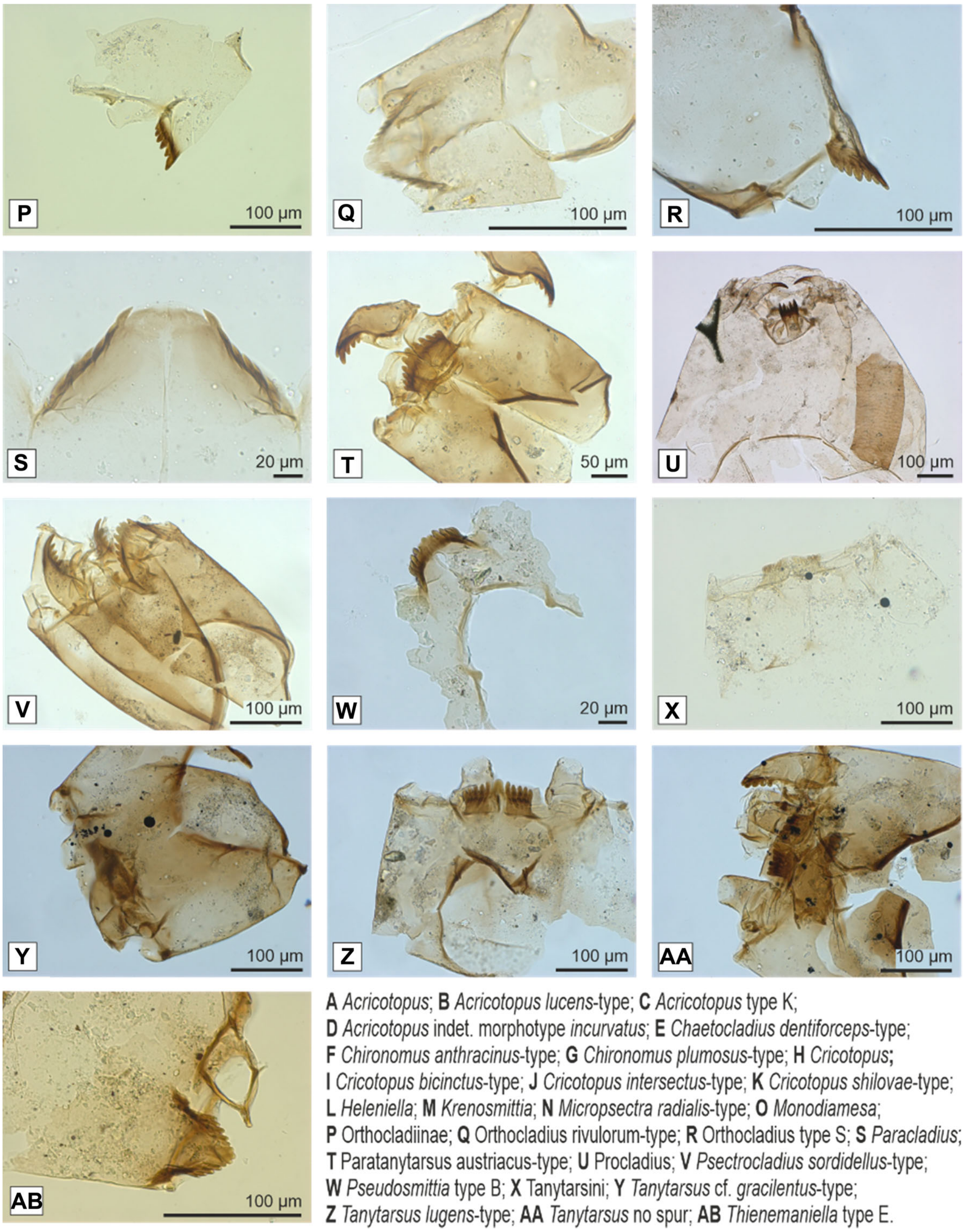

Figure 4. Continued

chironomid types at 7 cm depth (Fig. 6). Here, the curves for the rarefied taxa do not reach the asymptote (Fig. 5B). Therefore, the maximum number of chironomid types was not detected for this zone, indicating that we can expect a much larger number of taxa and therefore a higher diversity.

Relationship between chironomid assemblages and environmental variables

The NMDS shows the relationship between the chironomid assemblages and selected environmental variables based on their high variance percentages and *prior* knowledge (Fig. 7). Axis 1 (MDS1) is the most important axis explaining chironomid ordination. Considering only the most abundant chironomid taxa (abundances ≥2%), profundal taxa (*Micropsectra radialis*-type and *Paratanytarsus austriacus*-type) are associated with positive values of Axis MDS1, while *Chironomus* and *Procladius* are positioned towards the negative axis (Fig. 7). Most of the rare taxa (abundances <2%) are associated with littoral areas and are ordered towards the negative side of MDS1. Regarding environmental proxies, chironomid ordination in general is associated with Zr/Rb (13.54%), a grain size indicator (Dypvik and Harris 2001; Chen et al. 2006), followed by Sr/Ca (9.27) and Mg/Ca (3.26) (Table S3). TOC is more closely related to MDS2 (Fig. 7).

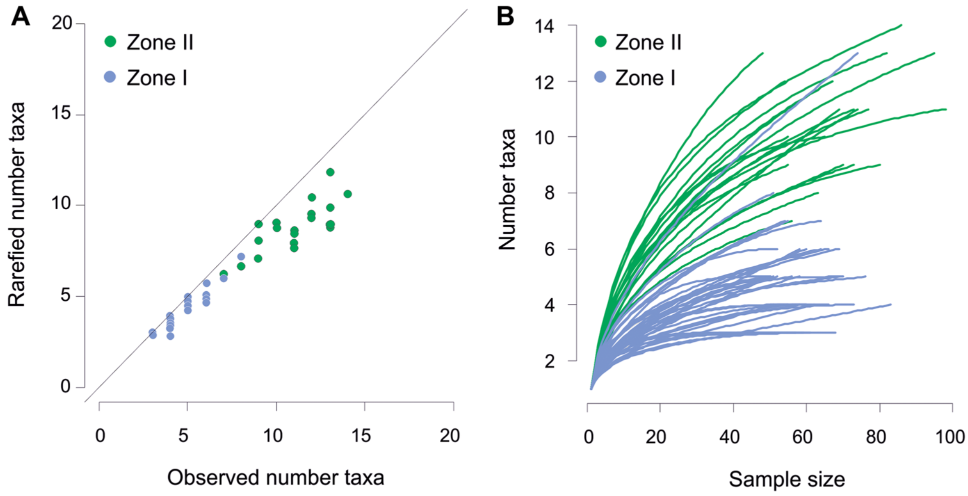

Figure 5. Rarefaction analysis for subfossil chironomid diversity. (A) Observed number of taxa vs. rarefied number of taxa. (B) Rarefaction curves per sample. Rarefied taxa reach the asymptote for Zone I, indicating that the maximum number of taxa in the sediment core was detected. Zone II did not reach the asymptote. [Color figure can be viewed at wileyonlinelibrary.com]

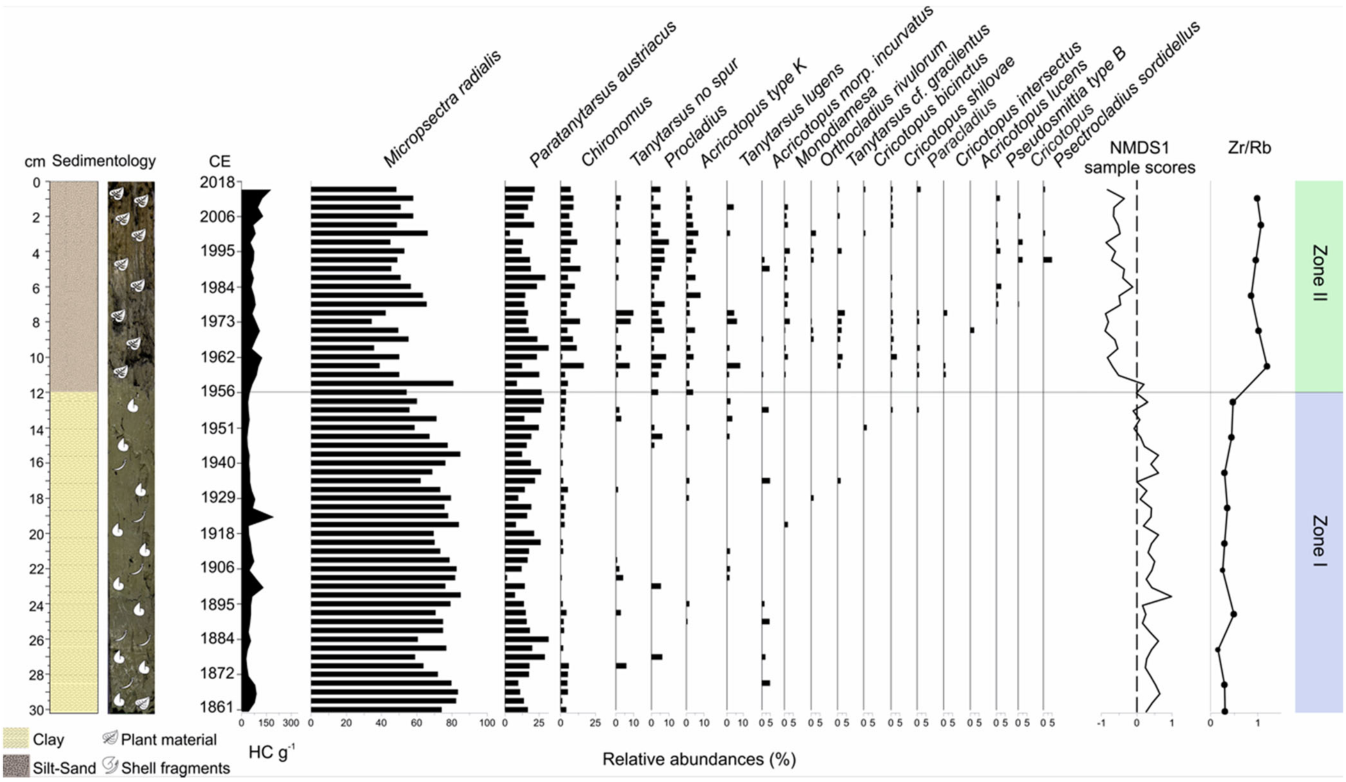

Figure 6. Chironomidae relative abundances of non-rare taxa (≥2%) from Lake Nam Co. HC g^{-1} denotes total number of head capsules. Sample scores from the first axis of the non-metric multidimensional scaling (NMDS1) and Zr/Rb changes, reflecting grain size, show Zone I with low diversity dominated by a cold-deep lake oligotrophic assemblage and small grain size; and Zone II with higher diversity and littoral-warm water-adapted taxa. [Color figure can be viewed at wileyonlinelibrary.com]

Discussion

Sub-fossil chironomid assemblage of Nam Co

The chironomid record of Nam Co is dominated by the *Micropsectra radialis*-type and the *Paratanytarsus austriacus*-type, two taxa associated with oligotrophic deep waters and low temperatures (Brooks et al., 2007; Kurek and Cwynar, 2009; Plank, 2010). A similar dominance was also observed in modern sediments of the high-altitudinal Tibetan lakes Taro Co (4566 m a.s.l.) (Laug et al., 2020), Heihai (4118 m a.s.l.) (Chang et al., 2017) and Tiancai (3900 m a.s.l.) (Zhang et al., 2017), where Tanytarsini morphotypes were highly abundant. In contrast, low species richness (*S*) was reported from sediment cores from Sugan Lake (*S* = 5 non-rare taxa) (Chen et al., 2009) and Heihai (*S* = 17 non-rare taxa) (Chang et al., 2017), northern TP, Shen Co, a shallow lake (*S* = 7 non-rare taxa) about 9 km north of Nam Co (Rigterink et al., 2022), and Son Kol, Kyrgyzstan (*S* = 10 non-rare taxa) (Laug et al., 2020). In Lake Tiancai, southwestern China, the richness of the most abundant chironomid taxon (*S* = 41) was the highest reported from a sediment core collected in high-altitude Central Asia (Zhang et al., 2017). Our Nam Co findings, however, represent the highest species richness (*S* = 25, 19 non-rare taxa) ever reported from a sediment core collected from the south-central TP.

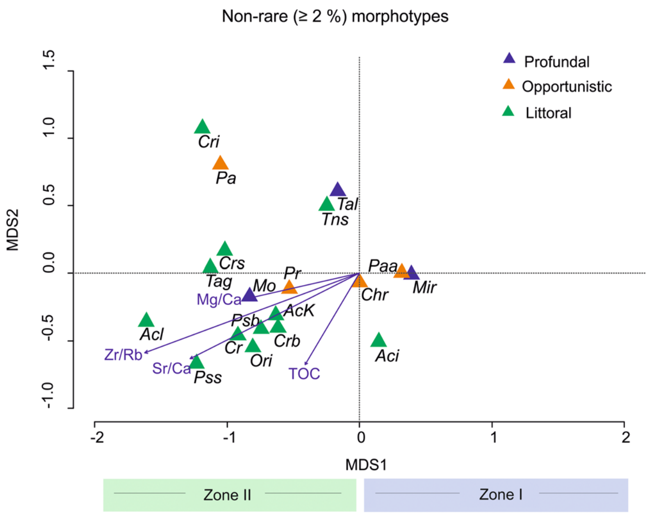

Figure 7. Non-metric multidimensional scaling analysis (NMDS) for chironomid assemblages (triangles) and most important environmental variables (arrows) to which taxa are associated. Zone I is characterized by profundal taxa, while Zone II is characterized by more littoral adapted taxa. Aci: *Acricotopus* indet. morphotype *incurvatus*, AcK: *Acricotopus* type K, Acl: *Acricotopus lucens*-type, Chr: *Chironomus*, Cr: *Cricotopus*, Crb: *Cricotopus bicinctus*-type, Cri: *Cricotopus intersectus*-type, Crs: *Cricotopus shilovae*-type, Mir: *Micropsectra radialis*-type, Mo: *Monodiamesa*, Ori: *Orthocladius rivolorum*-type, Pa: *Paracladius*, Paa: *Paratanytarsus austriacustype*, Pr: *Procladius*, Psb: *Pseudosmittia* type B., Pss: *Psectrocladius sordidellus*-type, Tag: *Tanytarsus* cf. *gracilentus*-type, Tal: *Tanytarsus lugens*-type, Tns: *Tanytarsus* no spur. [Color figure can be viewed at wileyonlinelibrary.com]

Since about 1956 CE, more warm-adapted taxa have been found (i.e. *Acricotopus lucens*-type, *Tanytarsus gracilentus*-type, *Orthocladius rivulorum*-type). The high diversity of the Orthocladiinae taxa during this period suggests an expansion of littoral habitats (Lods-Crozet et al., 2012; Brooks and Heiri, 2013). A similar chironomid taxon composition has been found in other high mountain lakes around the world (Rieradevall and Prat, 1999; Williams et al., 2019), where morphotypes (e.g. *Pseudosmittia* type B) were highly associated with semiterrestrial habitats and the presence of macrophytes (Brooks et al., 2007, Langdon et al., 2010; Moller Pillot, 2013). The synchronous establishment of *Chironomus plumosus*-type and *Procladius* with high abundances in Nam Co underlines their preference for mesotrophic to eutrophic conditions (Brooks et al., 2007; Tremblay et al., 2010; Araneda et al., 2013), suggesting that nutrients in the lake began to increase after about 1956 CE. This increase in primary productivity, however, is rather low and Nam Co can still be considered as being oligotrophic. This is supported by TN and TOC trends observed by that time (from 0.16 to 0.29% and 0.12 to 1.95%, respectively), in addition to the continuing dominance of the oligotrophic *Micropsectra radialis*-type and *Paratanytarsus austriacus*-type. High Zr/Rb ratios and increases of quartz and other silicate minerals (orthoclase, albite and epidote), which indicate high input of eroded sediments from the catchment, are consistent with higher runoff (Hamerlík et al., 2010). Increased runoff may cause turbulence and therefore transported sediments may damage HCs, thus hampering their identification (i.e. subfamilies Orthocladiinae and Tanytarsini, Fig. 4). By 1962 CE (10 cm depth), the decline in abundance of *Micropsectra radialis*-type causes major modifications in the chironomid community structure and more opportunistic and littoral adapted taxa have become present. This is the primary response of this taxon to higher water levels and, consequently, the expansion of littoral habitats. It took about 10 years for *Micropsectra radialis*-type to increase its abundance, but its abundances remained below the values during the previous period (1861–1956 CE). This was possibly caused by competitive pressure from other taxa, which influenced the availability of its ecological niche.

Different functional feeding groups characterize the chironomid assemblage and can be related to the ecological requirements of their larvae (Antczak-Orlewska et al., 2021). The feeding behavior is heavily influenced by different environmental features, such as changes in substrate and the entrance of organic matter. Ultimately, these factors have an impact on the availability and nutritional value of food sources (Silva et al., 2008). Prior to 1956 CE, only the collector-gatherer feeding group was represented by *Micropsectra radialis*-type, feeding on organic debris (Armitage et al. 1995). After 1956 CE, the species assemblage displays a higher diversity of species with feeding habits ranging from collector-gatherers to filter-feeders. Most of the functional feeding groups correspond to collector-gatherers, being mainly representatives of the subfamily Orthocladiinae, adapted to live in close contact with sediment, feeding on detritus, bacteria, protozoans, fungi and free-living algae (Moller Pillot, 2013). Only one predator was detected (*Procladius*) in higher abundances, indicating the availability of habitats that can harbor different microorganisms to be predated. The presence of *Cricotopus* and *Psectrocladius sordidellus*-type (Orthocladiinae), along with the filter-feeder *Monodiamesa* (Prodiamesinae), suggest a littoral habitat where macrophytes and unicellular algae are present (Pinder, 1986; Brooks et al., 2007). Previous studies have demonstrated that these habitats can also harbor opportunistic species (Henriques-Oliveira et al., 2003; Silva et al., 2008), and could be associated with an increasing supply of food particles carried by inflow after heavy rain events or by meltwater.

Environmental and hydrological changes

From 1861 to 1956 CE, the dominance of *Micropsectra radialis*-type and the low abundance of littoral taxa (i.e. *Acricotopus lucens*-type, *Tanytarsus gracilentus*-type, *Orthocladius rivulorum*-type) suggests a period of relatively stable, moderately high water levels. Stable Ti/Al and low Zr/Rb ratios, together with increased clay mineral contents, support the idea of a constant, moderate runoff. During this period, C/N ratios, a measure of the relative origin of organic matter (OM) accumulating in the lake, are low (<12), suggesting mainly autochthonous productivity (Wang et al., 2012; Kasper et al., 2013). Autochthonous OM sources have C/N ratios ranging between 4 and 12, because of the protein-rich and cellulose-poor composition of endogenous sources such as algae. OM originating from allochthonous sources in the catchment, on the other hand, show C/N ratios above 20 (Meyers, 2003; Wang et al., 2012). Between 1872 and 1884 CE, the slight decrease of *Micropsectra radialis*-type correlates with an increase of *Paratanytarsus austriacus*-type. Both taxa are adapted to deep water and suggest a decrease in available deep-water habitats. Indeed, around 1884 CE, higher values for low-Mg calcite and the increase of silicates, together with a decrease in clay minerals indicate that the environment was drier. Pulses of higher abundances of *Micropsectra radialis*-type at 29 and 24 cm (~1867 and ~1895 CE, respectively), together with higher C/N ratios and TOC, suggest short-lived inputs of material from the catchment. These pulses may have been indicative of stronger thaw periods (Kasper et al., 2012) or snow melt, transporting allochthonous material, including nutrients, into the lake. High C/N ratios between 1861 and 1895 CE indicate that macrophytes were always abundant, and also suggest a greater contribution of terrestrial organic matter from the basin (Wang et al., 2012).

Since 1956 CE, the increase of littoral taxa is accompanied by increasing levels of TN and phosphorus [P*(Zr/Rb)] and higher Ti/Al ratios. These factors reflect high nutrient supply driven by terrigenous riverine inputs from the Niya Qu. This is consistent with higher water levels and, consequently, the expansion of littoral habitats that causes aquatic plants to grow, providing suitable habitats for chironomids (Brodersen and Lindegaard, 1997; Langdon et al., 2010; Nazarova et al., 2017). Coarser grain sizes suggested by an increase in silt and sand are reflected by increasing Zr/Rb ratios, also indicative of increasing runoff from the Niya Qu. Rivers discharge more and coarser material into the lake during periods with higher precipitation rates and glacial meltwater input (Dypvik and Harris, 2001; Wang et al., 2015) possibly causing erosion from the carbonate-bearing rocks in the catchment of Nam Co. The increase in detrital input may have also increased ion concentration and favored the growth of authigenic MHC (Li et al. 2008; Li et al. 2009; Li et al. 2012) at the expense of low-Mg calcite, whereas dolomite has been mainly, if not entirely, of detrital origin (Li et al. 2008). The higher ion supply entering the lake has caused higher salinities, as reflected in higher Sr/Ca ratios. Previous studies on outcrops from Nam Co show a transition from a lacustrine to fluviolacustrine environment (Schütt et al., 2010). After the 1960s, higher abundances of deep-water ostracods found in short sediment cores suggest that water levels increased considerably (Wrozyna et al., 2010). The slightly higher values of TN measured in sediment core NC18-11b for the period between 1956 and 2018 CE are consistent with results from previous studies of surface sediment samples from the eastern part of the lake (Wang et al., 2012). The higher availability of TN, TOC and phosphate [P*(Zr/Rb)] resulting from supply of terrigenous material to the lake caused an increase in phytoplankton productivity. Consequently, abundances of hypoxia-tolerant taxa such as *Chironomus* and *Procladius* increased and suggest a decrease in hypolimnetic oxygen availability. Anoxic conditions at the lake floor are also supported by the presence of pyrite as well as elevated TOC/TN ratios as a consequence of increased preservation of organic matter due to increased productivity in the epilimnion and preservation of organic matter at the lake bottom. The increase of primary productivity in Nam Co was related to a longer growing period of macrophytes and shorter ice-cover duration for the last 100 years (Lami et al., 2010). Indeed, between 1965 and 2001 CE, the presence of the diatom *Stephanodiscus minutulus* is related to an increase in conductivity (Wang et al., 2011) and to longer thermal mixing phases during spring, influenced by strong monsoonal activity and abundant nutrient supply (Kasper et al., 2013). By 2006 CE, the decline of most elements and minerals in Nam Co sediments may be indicative of a decrease in runoff and increasing evaporation due to rising temperatures (Wang et al., 2011). Both decreasing runoff and increasing evaporation probably represent the dominant control of lake water level at decadal scales, while glacial meltwater, delivered at higher rates as a consequence of anthropogenic warming in recent years, is causing lake level fluctuations at annual temporal scales (Wang et al., 2011).

Our findings on the lake's nutrient and OM enrichment since 1956 CE underline the importance of alpine meadows around the lake. Herds of yaks, sheep and goats use these areas for grazing that promotes erosion, and, consequently, these meadows become another source of nutrients to the lake (Hopping et al., 2018; Anslan et al., 2020). Even though the lake is still oligotrophic, continued overgrazing in the area, along with the ongoing climate change, will cause drastic changes in the lake ecosystem. The most important consequence will be the increase in lake productivity that will modify the composition of chironomid assemblages and later other organisms inhabiting the lake, their timing and duration of successional, as well as modifications of the food-web structure within distinct successional stages (Straile, 2005).

Regional climate variability and potential forcing mechanisms

Our Nam Co sediment record covers the period known as the Current Warm Period (CWP). The CWP started at approximately 1850 CE and is characterized by a rise in temperatures after the Little Ice Age (LIA; about 1400 to about 1850 CE) (Matthews and Briffa, 2005; Neukom et al., 2019; Li et al., 2022). High-resolution records from Nam Co indicate a lake-level increase after the end of the LIA (Wrozyna et al., 2010; Günther et al., 2011). These results are consistent with studies by Denniston et al. (2000) and Chen et al. (2008), who suggested that ISM precipitation has increased over the past 1500 years, and that this trend was interrupted by the LIA (Denniston et al., 2000; Linderholm and Bräuning, 2006). From 1861 to 1956 CE, low chironomid diversity (rarefied mean number: six, mostly deep-water taxa) and stable to moderately high Ti/Al ratios suggest that temperatures were low, and, in general, little meltwater was produced. This may have been a stage during which the lake system was relatively stable, and deep-water chironomid communities were already well established. However, although conditions in the lake were relatively favorable, our sediment core suggests a drier environment around 1884 CE, with low values of clay minerals and high values of low-Mg calcite. This trend has been observed in different records such as ice cores, pollen, geochemistry and chironomids from sites relatively close to Nam Co that suggested a cold-dry climate (e.g. Thompson et al., 1989, 1997; Chen et al., 2009; Pu et al., 2013; Yang B. et al., 2014; Cui et al., 2021; Rigterink et al., 2022).

Since 1956 CE, a trend from cold-arid towards warm-wet conditions has been reported from the TP, especially for the central and eastern areas (Wu et al., 2007; Xu et al., 2008; Kuang and Jiao, 2016; Wang et al., 2018). Rising water levels of Nam Co have been detected since the 1970s, using remote sensing and GIS technologies (Zhu et al., 2010). However, in the multiproxy analysis presented here, we have detected considerable changes since 1956 CE. In Shen Co, a shallow lake located about 9 km north of Nam Co, chironomid composition as well as mineralogical and geochemical data from a short sediment core highlighted that after 1950 CE the water level rose (Rigterink et al., 2022). The increase in precipitation was attributed to a strong overlap of moisture supply from Westerly winds and the monsoon system (Rigterink et al., 2022). The climate data recorded from Qiantang, a meteorological station on the southern TP, show increasing trends of precipitation from 1961 to 2005 CE (Lu and Liu, 2010). This suggests that the catchment of Nam Co is especially sensitive to climate change and that the chironomid communities of lakes Nam Co and Shen Co are especially sensitive and respond early to environmental changes. Indeed, our combined results from chironomids and geochemical indicators suggest hydrological changes from moderately to high lake levels from 1861 to 1956 CE, to even higher water levels since 1956 CE. The progressive increase in lake levels has caused the expansion of littoral areas (Schütt et al., 2010) and more nutrients have entered the lake via the Niya Qu. Since the late 1970s, increasing runoff can be attributed to an earlier onset of summer precipitation (starting in May) due to ISM activity (Liu et al., 2019). This earlier onset triggers low-level South Westerlies anomalies over the northern Indian

Ocean, promoting moisture convergence and precipitation increase over the TP (Zhang et al., 2017). The stronger ISM could have accelerated the local water cycle, which may have also played an important role in the changes observed at Nam Co. High temperatures promote glacier melt, subsequently increasing runoff to the lake. There, lake water evaporates rapidly, causing the formation of clouds and finally local precipitation, restarting the cycle. Recent studies have shown that the observed warming on the TP is directly associated with the altered surface energy balance mainly related to the snow–albedo feedback and cloud–radiation interactions (Zhou and Zhang, 2021). A recent study has reported the detectable contribution of anthropogenic forcing to extreme temperature changes, including the increasing frequency of warm extremes and decreasing cold extremes on the eastern TP since 1958 CE (Yin et al., 2019). Therefore, it is important to highlight the effect of regional vs. seasonal changes in precipitation patterns of the TP. Thus, more meteorological data are needed to better understand the precipitation patterns on the high-altitude regions (Wang et al., 2018) to distinguish between the Indian monsoon influence and local water cycling.

Conclusions

This is the first paleoenvironmental study from the southern-central TP focusing on the last approximately 160 years that demonstrates the consequences that hydrological changes exert on the structure and diversity of chironomid communities. Two main periods were identified. (1) From 1861 to 1956 CE chironomid diversity was low and dominated by a cold and deep lake oligotrophic assemblage (e.g. *Micropsectra radialis*-type and *Paratanytarsus austriacus*-type). (2) Since 1956 CE diversity has increased, and species adapted to warm conditions, and high nutrient as well as low-oxygen tolerant taxa (i.e. *Chironomus*, *Procladius* and *Pseudosmittia* type B) became prominent. This ecological transformation is probably related to a change in lake and catchment hydrology, shifting from a moderate runoff and moderately to high lake levels with mainly autochthonous productivity to higher runoff and nutrient levels as well as an increase in terrigenous input. The presence of littoral Orthocladiinae indicates an expansion of littoral zones and the consequent increase of macrophyte belts. We suggest that these changes are primarily responses to an earlier onset of the ISM, which in turn enhances the local water cycle and water recycling. Increasing precipitation and runoff carry organic material and nutrients to the lake, shaping the chironomid assemblage composition and diversity. Even though Nam Co remains an oligotrophic lake, a slight increase in productivity has started to become apparent, since 1956 CE. In addition to the effects of ongoing climate change, overgrazing in the lake catchment as a human-induced disturbance factor additionally affects lake water quality. As shown by this study, chironomid assemblages are an ideal tool for monitoring and detecting changes in habitat availability and lake productivity, ultimately driven by anthropogenic warming.

Acknowledgments. We thank all the colleagues from the Institute of Tibetan Plateau Research and Nam Co Observation and Research Station (NAMORS) for their help during fieldwork in the Nam Co region. This research is a contribution to the International Research Training Group "Geo-ecosystems in transition on the Tibetan Plateau (TransTiP)", funded by Deutsche Forschungsgemeinschaft (DFG grant 317513741/GRK 2309). We acknowledge support by the Deutsche Forschungsgemeinschaft and the Open Access Publication Funds of the Technische Universität Braunschweig. Open Access funding enabled and organized by Projekt DEAL.

Author contributions—PGEG, LP and JM designed the study. WK, NB, AS and PP performed sampling. SR, AL and PGEG conducted Chironomidae analysis. BW established the age model. PH provided sediment-geochemical analyses and interpretation. JM, LP, LZ and ASchwalb revised and helped improve the manuscript. ASchwalb developed the programme (DFG GRK 2309/1) that funded this research. PGEG wrote the manuscript with contributions from all authors. All authors approved the final version.

Conflict of interest—The authors declare no competing interests.

Data availability statement

Data available in article supplementary material.

Supporting information

Additional supporting information can be found in the online version of this article.

Abbreviations. ASM, Asian summer monsoon; CE, common era; CONISS, stratigraphically constrained cluster analysis; CWP, Current Warm Period; DOM, dissolved organic matter; EASM, East Asian summer monsoon; HC, head capsule; ICDD, International Centre for Diffraction Data; ISM, Indian summer monsoon; LIA, Little Ice Age; MHC, monohydrocalcite; NAMORS, Nam Co Monitoring and Research Station for Multisphere Interactions; NAMORS, Nam Co Observation and Research Station; NMDS, non-metric multidimensional scaling; OM, organic matter; P-ED XRF, X-ray fluorescence spectrometer; *S*, species richness; SAR, sediment accumulation rate; TC, total carbon; TIC, total inorganic carbon; TN, total nitrogen; TOC, total organic carbon; TP, Tibetan Plateau; TransTiP, International Research Training Group "Geo-ecosystems in transition on the Tibetan Plateau; XRD, X-ray diffraction.

References

Abril, J.M. (2004) Constraints on the use of ^{137}Cs as a time-marker to support CRS and SIT chronologies. *Environmental Pollution*, 129, 31–37.

Anslan, S., Azizi Rad, M., Buckel, J., Echeverria Galindo, P., Kai, J., Kang, W. et al. (2020) Reviews and syntheses: How do abiotic and biotic processes respond to climatic variations in the Nam Co catchment (Tibetan Plateau)? *Biogeosciences*, 17, 1261–1279.

Antczak-Orlewska, O., Płóciennik, M., Sobczyk, R., Okupny, D., Stachowicz-Rybka, R., Rzodkiewicz, M. et al. (2021) Chironomidae morphological types and functional feeding groups as a habitat complexity vestige. *Frontiers in Ecology and Evolution*, 8, 583831. https://doi.org/10.3389/fevo.2020.583831

Appleby, P.G. (2008) Three decades of dating recent sediments by fallout radionuclides: a review. *The Holocene*, 18, 83–93.

Appleby, P.G., Nolan, P.J., Gifford, D.W., Godfrey, M.J., Oldfield, F., Anderson, N.J. et al. (1986) ^{210}Pb dating by low background gamma counting. *Hydrobiologia*, 143, 21–27.

Appleby, P.G. & Oldfield, F. (1978) The calculation of lead-210 dates assuming a constant rate of supply of unsupported 210Pb to the sediment. *Catena*, 5, 1–8.

Araneda, A., Jana, P., Ortega, C., Torrejo, F., Bertrand, S., Vargas, P. et al. (2013) Changes in sub-fossil chironomid assemblages in two northern patagonian lake systems associated with the occurrence of historical fires. *Journal of Paleolimnology*, 50, 41–56.

Armitage, P.D., Cranston, P.S. & Pinder, L.C.V. (1995) The chironomidae, In: *Biology and ecology of non-biting chironomids*. London: Chapman & Hall.

Battarbee, R.W. (2000) Palaeolimnological approaches to climate change, with special regard to the biological record. *Quaternary Science Reviews*, 19, 107–124.

Bengtsson, L. (1996) Mixing in ice-covered lakes. In: *The First International Lake Ladoga Symposium*. https://doi.org/10.1007/978-94-009-1655-5_14

Bennett, K.D. (1996) Determination of the number of zones in a biostratigraphical sequence. *New Phytologist*, 132, 155–170.

Bitušík, P. & Hamerlík, L. (2014) Príručka na určovanie lariev pakomárov (Diptera: Chironomidae) Slovenska Časť 2. Tanypodinae. [Identification guide of Slovakian chironomid larvae (Diptera: Chironomidae). Part II. Tanypodinae]. [Book in Slovak]. Belianum. Matej Bel University Publ., Banská Bystrica. p. 96.

Bolch, T., Yao, T., Kang, S., Buchroithner, M.F., Scherer, D., Maussion, F. et al. (2010) A glacier inventory for the western Nyainqentanglha Range and the Nam Co Basin, Tibet, and glacier changes 1976–2009. *The Cryosphere*, 4, 419–433.

Brodersen, K.P. & Lindegaard, C. (1997) Significance of subfossile chironomid remains in classification of shallow lakes. *Hydrobiologia*, 342/343, 125–132.

Brooks, S.J. (2006) Fossil midges (Diptera: Chironomidae) as palaeoclimatic indicators for the Eurasian region. *Quaternary Science Reviews*, 25, 1894–1910.

Brooks, S.J. & Heiri, O. (2013) Response of chironomid assemblages to environmental change during the early Late-glacial at Gerzensee, Switzerland. *Palaeogeography, Palaeoclimatology, Palaeoecology*, 391, 90–98.

Brooks, S.J., Langdon, P.G. & Heiri, O. (2007) *The Identification and Use of Palaearctic Chironomidae Larvae in Palaeoecology*. London: Quaternary Research Association. p. 276.

Chang, J., Zhang, E., Liu, E. & Shulmeister, J. (2017) Summer temperature variability inferred from subfossil chironomid assemblages from the south-east margin of the Qinghai–Tibetan Plateau for the last 5000 years. *The Holocene*, 27, 1876–1884.

Chen, F., Yu, Z., Yang, M., Ito, E., Wang, S., Madsen, D.B. et al. (2008) Holocene moisture evolution in arid central Asia and its out-of-phase relationship with Asian monsoon history. *Quaternary Science Reviews*, 27(3-4), 351–364. https://doi.org/10.1016/j.quascirev.2007.10.017

Chen, J., Chen, F., Zhang, E., Brooks, S.J., Zhou, A. & Zhang, J. (2009) A 1000-year chironomid-based salinity reconstruction from varved sediments of Sugan Lake, Qaidam Basin, arid Northwest China, and its palaeoclimatic significance. *Chinese Science Bulletin*, 54, 3749–3759.

Chen, J., Chen, Y., Liu, L., Ji, J., Balsam, W., Sun, Y. et al. (2006) Zr/Rb ratio in the Chinese loess sequences and its implication for changes in the East Asian winter monsoon strength. *Geochimica et Cosmochimica Acta*, 70(6), 1471–1482.

Cui, A., Lu, H., Liu, X., Shen, C., Xu, D., Xu, B. et al. (2021) Tibetan Plateau precipitation modulated by the periodically coupled Westerlies and Asian Monsoon. *Geophysical Research Letters*, 48, e2020GL091543.

Denniston, R.F., Gonzalez, L.A., Asmerom, Y., Sharma, R.H. & Reagan, M.K. (2000) Speleothem evidence for changes in Indian summer monsoon precipitation over the last ~2300 years. *Quaternary Research*, 53, 196–202.

Doberschütz, S., Frenzel, P., Haberzettl, T., Kasper, T., Wang, J., Zhu, L. et al. (2014) Monsoonal forcing of Holocene paleoenvironmental change on the central Tibetan Plateau inferred using a sediment record from Lake Nam Co (Xizang, China). *Journal of Paleolimnology*, 51, 253–266.

Dypvik, H. & Harris, N.B. (2001) Geochemical facies analysis of fine-grained siliciclastics using Th/U, Zr/Rb and (Zr+Rb)/Sr ratios. *Chemical Geology*, 181, 131–146.

Eggermont, H. & Heiri, O. (2012) The chironomid-temperature relationship: expression in nature and palaeoenvironmental implications. *Biological Reviews*, 87, 430–456.

Engels, S., Medeiros, A.S., Axford, Y., Brooks, S.J., Heiri, O., Luoto, T.P. et al. (2020) Temperature change as a driver of spatial patterns and long-term trends in chironomid (Insecta: Diptera) diversity. *Global Change Biology*, 26, 1155–1169.

Fang, Y., Cheng, W., Zhang, Y., Wang, N., Zhao, S., Zhou, C. et al. (2016) Changes in inland lakes on the Tibetan Plateau over the past 40 years. *Journal of Geographical Sciences*, 26, 415–438.

Golosov, S., Maher, O.A., Schipunova, E., Terzhevik, A., Zdorovennova, G. & Kirillin, G. (2006) Physical background of the development of oxygen depletion in ice-covered lakes. *Oecologia*, 151(2), 331–340. https://doi.org/10.1007/s00442-006-0543-8

Grimm, E.C. (1987) CONISS: A Fortran 11 program for stratigraphically constrained cluster analysis by the method of incremental cluster analysis by the method of incremental sum of squares. *Computers and Geoscience*, 13, 13–35.

Günther, F., Mügler, I., Mäusbacher, R., Daut, G., Leopold, K., Gerstmann, U.C. et al. (2011) Response of δD values of sedimentary n-alkanes to variations in source water isotope signals and climate proxies at Lake Nam Co, Tibetan Plateau. *Quaternary International*, 236, 82–90.

Hamerlík, L., Christoffersen, K.S. & Brodersen, K.P. (2010) Short comment on chironomid assemblages and stratigraphy of high altitude lakes from tibet. *CHIRONOMUS Journal of Chironomidae Research*, 23, 20–24.

Henriques-Oliveira, A.L., Nessimian, J.L. & Dorvillé, L.F.M. (2003) Feeding habits of chironomid larvae (Insecta: Diptera) from a stream in the Floresta da Tijuca, Rio de Janeiro, Brazil. *Brazilian Journal of Biology*, 63, 269–281.

Hopping, K.A., Knapp, A.K., Dorji, T. & Klein, J.A. (2018) Warming and land use change concurrently erode ecosystem services in Tibet. *Global Change Biology*, 24(11), 5534–5548. https://doi.org/10.1111/gcb.14417

Hua, Q., Barbetti, M. & Rakowski, A. (2013) Atmospheric Radiocarbon for the Period 1950–2010. *Radiocarbon*, 55(4), 2059-2072. doi:10.2458/azu_js_rc.v55i2.16177

Huang, L., Wang, J., Zhu, L., Ju, J. & Daut, G. (2017) The Warming of Large Lakes on the Tibetan Plateau: Evidence From a Lake Model Simulation of Nam Co, China, During 1979-2012. *Journal of Geophysical Research: Atmospheres*, 122, 13,095–13,107.

Jiang, L., Nielsen, K., Andersen, O.B. & Bauer-Gottwein, P. (2017) Monitoring recent lake level variations on the Tibetan Plateau using CryoSat-2 SARIn mode data. *Journal of Hydrology*, 544, 109–124.

Juggins, S. (2007) C2. Newcastle University, Newcastle upon Tyne, UK.

Kai, J., Wang, J., Ju, J., Huang, L., Ma, Q., Daut, G. et al. (2020) Spatio-temporal variations of hydrochemistry and modern sedimentation processes in the Nam Co basin, Tibetan Plateau: Implications for carbonate precipitation. *Journal of Great Lakes Research*, 46, 961–975.

Kasper, T., Frenzel, P., Haberzettl, T., Schwarz, A., Daut, G., Meschner, S. et al. (2013) Interplay between redox conditions and hydrological changes in sediments from Lake Nam Co (Tibetan Plateau) during the past 4000 cal BP inferred from geochemical and micropaleontological analyses. *Palaeogeography, Palaeoclimatology, Palaeoecology*, 392, 261–271.

Kasper, T., Haberzettl, T., Doberschütz, S., Daut, G., Wang, J., Zhu, L. et al. (2012) Indian ocean summer monsoon (IOSM)-dynamics within the past 4 ka recorded in the sediments of Lake Nam Co, central Tibetan Plateau (China). *Quaternary Science Reviews*, 39, 73e85.

Keil, A., Berking, J., Mügler, I., Schütt, B., Schwalb, A. & Steeb, P. (2010) Hydrological and geomorphological basin and catchment characteristics of Lake Nam Co, South-Central Tibet. *Quaternary International*, 218, 118–130.

Kenkel, N.C. & Orloci, L. (1986) Applying Metric and Nonmetric Multidimensional Scaling to Ecological Studies: Some New Results. *Ecology*, 67, 919–928.

Kuang, X. & Jiao, J.J. (2016) Review on climate change on the Tibetan Plateau during the last half century. *Journal of Geophysical Research: Atmospheres*, 121, 3979–4007. Available at https://doi.org/10.1002/2015JD024728

Kurek, J. & Cwynar, L.C. (2009) Effects of within-lake gradients on the distribution of fossil chironomids from maar lakes in western Alaska: implications for environmental reconstructions. *Hydrobiologia*, 623, 37–52.

Kylander, M.E., Ampel, L., Wohlfarth, B. & Veres, D. (2011) High-resolution X-ray fluorescence core scanning analysis of Les Echets (France) sedimentary sequence: new insights from chemical proxies: XRF CORE SCANNING ANALYSIS OF LES ECHETS SEDIMENTARY SEQUENCE. *Journal of Quaternary Science*, 26(1), 109–117.

Lami, A., Turner, S., Musazzi, S., Gerli, S., Guilizzoni, P., Rose, N.L. et al. (2010) Sedimentary evidence for recent increases in production in Tibetan plateau lakes. *Hydrobiologia*, 648, 175–187.

Langdon, P., Ruiz, Z., Wynne, S., Sayer, C. & Davidson, T. (2010) Ecological influences on larval chironomid communities in shallow lakes: implications for paleolimnological interpretations. *Freshwater Biology*, 55, 531–545.

Laug, A., Hamerlík, L., Anslan, S., Engels, S., Turner, F., Wang, J. et al. (2019) Acricotopus indet. morphotype incurvatus: Description and genetics of a new Orthocladiinae (Diptera: Chironomidae) larval morphotype from the Tibetan Plateau. *Zootaxa*, 4656, 535–544. https://doi.org/10.11646/zootaxa.4656.3.10

Laug, A., Turner, F., Engels, S., Wang, J., Haberzettl, T., Ju, J. et al. (2020) Is there a common threshold to subfossil chironomid assemblages at 16 m water depth? Evidence from the Tibetan Plateau: 16 m water depth – a chironomid depth threshold? *Journal of Limnology*, 79(3), 278–292.

Lei, Y., Yao, T., Bird, B.W., Yang, K., Zhai, J. & Sheng, Y. (2013) Coherent lake growth on the central Tibetan Plateau since the 1970s: Characterization and attribution. *Journal of Hydrology*, 483, 61–67.

Lei, Y., Yang, K., Wang, B., Sheng, Y., Bird, B.W., Zhang, G. et al. (2014) Response of inland lake dynamics over the Tibetan Plateau to climate change. *Climatic Change*, 125, 281–290.

Li, M., Wang, J., Zhu, L., Wang, L. & Yi, C. (2012) Distribution and formation of monohydrocalcite from surface sediments in Nam Co Lake, Tibet. *Quaternary International*, 263, 85–92.

Li, M., Kang, S., Zhu, L., You, Q., Zhang, Q. & Wang, J. (2008) Mineralogy and geochemistry of the Holocene lacustrine sediments in Nam Co, Tibet. *Quaternary International*, 187, 105–116.

Li, M., Kang, S., Zhu, L., Wang, F., Wang, J., Yi, C. et al. (2009) On the Unusual Holocene Carbonate sediment in Lake Nam Co, Central Tibet. *Journal of Mountain Science*, 6, 346–353.

Li, M., Zheng, M., Ye, C., Wang, C., Zhang, X., Wang, X. et al. (2022) Response of travertine dam to precipitation over the past 800 years in Zabuye salt Lake, southwestern Tibetan Plateau. *Minerals*, 12(7), 916. Available at https://doi.org/10.3390/min12070916

Linderholm, H.W. & Bräuning, A. (2006) Comparison of high-resolution climate proxies from the Tibetan plateau and Scandinavia during the last millennium. *Quaternary International*, 154–155, 141–148.

Liu, X., Zhang, X., Lin, Y., Jin, L. & Chen, F. (2019) Strengthened Indian summer monsoon brought more rainfall to the western Tibetan Plateau during the early Holocene. *Science Bulletin*, 64(20), 1482–1485. Available at https://doi.org/10.1016/j.scib.2019.07.022

Lockot, G., Ramisch, A., Wünnemann, B., Hartmann, K., Haberzettl, T., Chen, H. et al. (2015) A Process- and Provenance-Based Attempt to Unravel Inconsistent Radiocarbon Chronologies in Lake Sediments: An Example from Lake Heihai, North Tibetan Plateau (China). *Radiocarbon*, 57(5), 1003–1019.

Lods-Crozet, B., Oertli, B. & Robinson, C.T. (2012) Long-term patterns of chironomid assemblages in a high elevation stream/lake network (Switzerland)—implications to global change. *Fauna Norvegica*, 31, 71–85.

Lu, H. & Liu, G. (2010) Trends in temperature and precipitation on the Tibetan Plateau, 1961–2005. *Climate Research*, 43(3), 179–190. http://www.jstor.org/stable/24870361

Luoto, T.P. (2010) Hydrological change in lakes inferred from midge assemblages through use of an intralake calibration set. *Ecological Monographs*, 80, 303–329.

Ma, N., Szilagyi, J., Niu, G.-Y., Zhang, Y., Zhang, T., Wang, B. et al. (2016) Evaporation variability of Nam Co Lake in the Tibetan Plateau and its role in recent rapid lake expansion. *Journal of Hydrology*, 537, 27–35.

Mathias, J.A. & Barica, J. (1980) Factors controlling oxygen depletion in ice-covered lakes. *Canadian Journal of Fisheries and Aquatic Sciences*, 37(2), 185–194. https://doi.org/10.1139/f80-024

Matthews, J.A. & Briffa, K.R. (2005) The ‘Little Ice Age’: Reevaluation of an evolving concept. *Geografiska Annaler: Series A, Physical Geography*, 87A, 17–36.

Meyers, P.A. (2003) Applications of organic geochemistry to paleolimnological reconstructions: a summary of examples from the Laurentian Great Lakes. *Organic Geochemistry*, 34, 261–289.

Mischke, S., Weynell, M., Zhang, C. & Wiechert, U. (2013) Spatial variability of 14C reservoir effects in Tibetan Plateau lakes. *Quaternary International*, 313-314, 147–155.

Moller Pillot, H.K.M. (2013) *Chironomidae Larvae, Vol. 3: Orthocladiinae*. Leiden, Niederlande: KNNV Publishing. Available at https://doi.org/10.1163/9789004278059

Morrill, C. (2004) The influence of Asian summer monsoon variability on the water balance of a Tibetan lake. *Journal of Paleolimnology*, 32, 273–286.

Mügler, I., Gleixner, G., Günther, F., Mäusbacher, R., Daut, G., Schütt, B. et al. (2010) A multi-proxy approach to reconstruct hydrological changes and Holocene climate development of Nam Co, Central Tibet. *Journal of Paleolimnology*, 43, 625–648.

Nazarova, L., Bleibtreu, A., Hoff, U., Dirksen, V. & Diekmann, B. (2017) Changes in temperature and water depth of a small mountain lake during the past 3000 years in Central Kamchatka reflected by a chironomid record. *Quaternary International*, 447, 46–58.

Nazarova, L., Self, A.E., Brooks, S.J., van Hardenbroek, M., Herzschuh, U. & Diekmann, B. (2015) Northern Russian chironomid-based modern summer temperature data set and inference models. *Global and Planetary Change*, 134, 10–25.

Neukom, R., Steiger, N., Gómez-Navarro, J.J., Wang, J. & Werner, J.P. (2019) No evidence for globally coherent warm and cold periods over the preindustrial Common Era. *Nature*, 571, 550–554. Available at https://doi.org/10.1038/s41586-019-1401-2

Pinder, L.C.V. (1986) Biology of Freshwater Chironomidae. *Annual Review of Entomology*, 31, 1–23.

Plank, A., 2010. Chironomid-based inference models for Tibetan lakes aided by a newly developed chironomid identification key. Berlin: 171 pp.

Pu, Y., Nace, T., Meyers, P.A., Zhang, H., Wang, Y., Zhang, C.L. et al. (2013) Paleoclimate changes of the last 1000 yr on the eastern Qinghai–Tibetan Plateau recorded by elemental, isotopic, and molecular organic matter proxies in sediment from glacial Lake Ximencuo. *Palaeogeography, Palaeoclimatology, Palaeoecology*, 379-380, 39–53.

Raposeiro, P.M., Saez, A., Giralt, S., Costa, A.C. & Gonçalves, V. (2018) Causes of spatial distribution of subfossil diatom and chironomid assemblages in surface sediments of a remote deep island lake. *Hydrobiologia*, 815, 141–163.

Reimer, P., Austin, W., Bard, E., Bayliss, A., Blackwell, P., Bronk Ramsey, C. et al. (2020) The IntCal20 northern hemisphere radiocarbon age calibration curve (0–55 cal kBP). *Radiocarbon*, 62(4), 725–757. https://doi.org/10.1017/RDC.2020.41

Rieradevall, M. & Prat, N. (1999) Chironomidae from high mountain lakes in Spain and Portugal. In: Hoffrichter, O. (Ed.) *Late 20th century research on Chironomidae: an anthology from the 13th International Symposium on Chironomidae*. Shaker Verlag. pp. 605–613.

Rigterink, S., Echeverría-Galindo, P., Martínez-Abarca, R., Massaferro, J., Hoelzmann, P., Wünnemann, B. et al. (2022) Sub-Fossil Chironomids as Indicators of Hydrological Changes in the Shallow and High-Altitude Lake Shen Co, Tibetan Plateau, over the past Two Centuries. *Journal of Limnology*, 81. Available at https://doi.org/10.4081/jlimnol.2022.2077

Rue, G.P., Darling, J.P., Graham, E., Tfaily, M.M. & McKnight, D.M. (2019) Dynamic changes in dissolved organic matter composition in a Mountain Lake under ice cover and relationships to changes in nutrient cycling and phytoplankton community composition. *Aquatic Sciences*, 82, 15. Available at https://doi.org/10.1007/s00027-019-0687-3

Schütt, B., Berking, J., Frechen, M., Frenzel, P., Schwalb, A. & Wrozyna, C. (2010) Late Quaternary transition from lacustrine to a fluvio-lacustrine environment in the north-western Nam Co, Tibetan Plateau, China. *Quaternary International*, 218, 104–117.

Silva, F.L., Ruiz, S., Bochini, G.L. & Moreira, D.C. (2008) Functional feeding habits of Chironomidae larvae (Insecta, Diptera) in a lotic system from Midwestern region of São Paulo State, Brazil. *Pan-American Journal of Aquatic Sciences*, 3, 135–141.

Spencer, R.G.M., Guo, W., Raymond, P.A., Dittmar, T., Hood, E., Fellman, J. et al. (2014) Source and biolability of ancient dissolved organic matter in glacier and lake ecosystems on the Tibetan Plateau. *Geochimica et Cosmochimica Acta*, 142, 64–74. Available at https://doi.org/10.1016/j.gca.2014.08.006

Straile, D. (2005). Food webs in lakes, seasonal dynamics and the impact of climate variability. ed. Andrea Belgrano. Oxford University Press. 41-50. https://d-nb.info/1095781081/34

Su, F., Duan, X., Chen, D., Hao, Z. & Cuo, L. (2013) Evaluation of the Global Climate models in the CMIP5 over the Tibetan Plateau. *Journal of Climate*, 26, 3187–3208.

Sun, J., Yang, K., Guo, W., Wang, Y., He, J. & Lu, H. (2020) Why Has the Inner Tibetan Plateau become wetter since the mid-1990s? *Journal of Climate*, 33, 8507–8522.

Thompson, L.G., Mosley-Thompson, E., Davis, M.E., Bolzan, J.F., Dai, J., Klein, L. et al. (1989) Holocene-late pleistocene climatic ice core records from Qinghai-Tibetan Plateau. *Science*, 246, 474–477.

Thompson, L.G., Yao, T., Davis, M.E., Henderson, K.A., Mosley-Thompson, E., Lin, P.-N. et al. (1997) Tropical climate instability: The last glacial cycle from a Qinghai-Tibetan ice core. *Science*, 276, 1821–1825.

Tremblay, V., Larocque, I. & Sirois, P. (2010) Historical variability of subfossil chironomids (Diptera:Chironomidae) in three lakes impacted by natural and anthropogenic disturbances. *Journal of Paleolimnology*, 44(2), 483–495. https://doi.org/10.1007/s10933-010-9429-1

Walker, I.R. (1987) Chironomidae (Diptera) in Paleoecology. *Quaternary Science Reviews*, 6, 29–40.

Walther, G.R. (2010) Community and ecosystem responses to recent climate change. *Philosophical Transactions of the Royal Society B: Biological Sciences*, 365, 2019–2024. https://doi.org/10.1098/rstb.2010.0021

Wang, C. & Morrison, R.J. (2014) Phosphorus speciation and changes with depth in the sediment of Lake Illawarra, New South Wales, Australia. *Environmental Earth Sciences*, 71, 3529–3541. https://doi.org/10.1007/s12665-013-2742-z

Wang, J., Huang, L., Ju, J., Daut, G., Wang, Y., Ma, Q. et al. (2019) Spatial and temporal variations in water temperature in a high-altitude deep dimictic mountain lake (Nam Co), central Tibetan Plateau. *Journal of Great Lakes Research*, 45, 212–223. Available at https://doi.org/10.1016/j.jglr.2018.12.005

Wang, J., Huang, L., Ju, J., Daut, G., Ma, Q., Zhu, L. et al. (2020) Seasonal stratification of a deep, high-altitude, dimictic lake: Nam Co, Tibetan Plateau. *Journal of Hydrology*. Available at https://doi.org/10.1016/j.jhydrol.2020.124668

Wang, J., Zhu, L., Wang, Y., Ju, J., Daut, G. & Li, M. (2015) Spatial variability and the controlling mechanisms of surface sediments from Nam Co, central Tibetan Plateau, China. *Sedimentary Geology*, 319, 69–77.

Wang, R., Yang, X., Langdon, P. & Zhang, E. (2011) Limnological responses to warming on the Xizang Plateau, Tibet, over the past 200 years. *Journal of Paleolimnology*, 45, 257–271.

Wang, X., Pang, G. & Yang, M. (2018) Precipitation over the Tibetan Plateau during recent decades:a review based on observations and simulations. *International Journal of Climatology*, 38, 1116–1131.

Wang, Y., Zhu, L., Wang, J., Ju, J. & Lin, X. (2012) The spatial distribution and sedimentary processes of organic matter in surface sediments of Nam Co, Central Tibetan Plateau. *Chinese Science Bulletin*, 57, 4753–4764.

Williams, N., Añón Suárez, D., Rieradevall, M., Rizzo, A., Daga, R., Arribére, M.A. et al. (2019) Response of chironomidae to environmental disturbances in a high mountain lake in Patagonia during the last millennium. *Quaternary Research*, 92, 273–287. https://doi.org/10.1017/qua.2019.5

Wrozyna, C., Frenzel, P., Steeb, P., Zhu, L., van Geldern, R., Mackensen, A. et al. (2010) Stable isotope and ostracode species assemblage evidence for lake level changes of Nam Co, southern Tibet, during the past 600years. *Quaternary International*, 212, 2–13.

Wu, K., Zhao, W., Li, M., Picazo, F., Soininen, J., Shen, J. et al. (2020) Taxonomic dependency of beta diversity components in benthic communities of bacteria, diatoms and chironomids along a water-depth gradient. *Science of the Total Environment*, 741, 140462.

Wu, S., Yin, Y., Zheng, D. & Yang, Q. (2007) Climatic trends over the Tibetan Plateau during 1971–2000. *Journal of Geographical Sciences*, 17, 141–151.

Wünnemann, B., Yan, D., Andersen, N., Riedel, F., Zhang, Y., Sun, Q. et al. (2018) A 14 ka high-resolution δ18O lake record reveals a paradigm shift for the process-based reconstruction of hydroclimate on the northern Tibetan Plateau. *Quaternary Science Reviews*, 200, 65–84.

Xu, Z.X., Gong, T.L. & Li, J.Y. (2008) Decadal trend of climate in the Tibetan Plateau – regional temperature and precipitation. *Hydrological Processes*, 22, 3056–3065.

Yang, K., Ye, B., Zhou, D., Wu, B., Foken, T., Qin, J. et al. (2011) Response of hydrological cycle to recent climate changes in the Tibetan Plateau. *Climatic Change*, 109, 517–534.

Yang, K., Wu, H., Qin, J., Lin, C., Tang, W. & Chen, Y. (2014) Recent climate changes over the Tibetan Plateau and their impacts on energy and water cycle: A review. *Global and Planetary Change*, 112, 79–91.

Yang, B., Qin, C., Wang, J., He, M., Melvin, T.M., Osborn, T.J. et al. (2014) A 3,500-year tree-ring record of annual precipitation on the northeastern Tibetan Plateau. *Proceedings of the National Academy of Sciences of the United States of America*, 111, 2903–2908.

Yang, R., Zhu, L., Wang, J., Ju, J., Ma, Q., Turner, F. et al. (2017) Spatiotemporal variations in volume of closed lakes on the Tibetan Plateau and their climatic responses from 1976 to 2013. *Climatic Change*, 140, 621–633.

Yao, T., Bolch, T., Chen, D., Gao, J., Immerzeel, W., Piao, S. et al. (2022) The imbalance of the Asian water tower. *Nature Reviews Earth & Environment*, 3, 618–632. Available at https://doi.org/10.1038/s43017-022-00299-4

Yao, T., Masson-Delmotte, V., Gao, J., Yu, W., Yang, X., Risi, C. et al. (2013) A review of climatic controls on δ18O in precipitation over the Tibetan Plateau: Observations and simulations: TP PRECIPITATION STABLE ISOTOPES. *Reviews of Geophysics*, 51, 525–548.

Yao, T., Pu, J., Lu, A., Wang, Y., & Yu, W. (2007) Recent glacial retreat and its impact on hydrological processes on the Tibetan Plateau, China, and surrounding regions. *Arctic, Antarctic, and Alpine Research*, 39, 642–650, https://doi.org/10.1657/1523-0430(07-510)[YAO]2.0.CO;2

Yin, H., Sun, Y. & Donat, M.G. (2019) Changes in temperature extremes on the Tibetan Plateau and their attribution. *Environmental Research Letters*, 14, 124015.

Zhang, E., Chang, J., Cao, Y., Tang, H., Langdon, P., Shulmeister, J. et al. (2017) A chironomid-based mean July temperature inference model from the south-east margin of the Tibetan Plateau, China. *Climate of the Past*, 13, 185–199.

Zhang, G., Xie, H., Kang, S., Yi, D. & Ackley, S.F. (2011) Monitoring lake level changes on the Tibetan Plateau using ICESat altimetry data (2003–2009). *Remote Sensing of Environment*, 115, 1733–1742.

Zhang, J., Hu, Q., Li, Y., Li, H. & Li, J. (2021) Area, lake-level and volume variations of typical lakes on the Tibetan Plateau and their response to climate change, 1972–2019. *Geo-spatial Information Science*, 24, 458–473.

Zhou, S., Kang, S., Chen, F. & Joswiak, D.R. (2013) Water balance observations reveal significant subsurface water seepage from Lake Nam Co, south-central Tibetan Plateau. *Journal of Hydrology*, 491, 89–99.

Zhou, T. & Zhang, W. (2021) Anthropogenic warming of Tibetan Plateau and constrained future projection. *Environmental Research Letters*, 16, 044039.

Zhu, L., Wu, Y., Wang, J., Lin, X., Ju, J., Xie, M. et al. (2008) Environmental changes since 8.4ka reflected in the lacustrine core sediments from Nam Co, central Tibetan Plateau, China. *The Holocene*, 18, 831–839.

Zhu, L., Xie, M. & Wu, Y. (2010) Quantitative analysis of lake area variations and the influence factors from 1971 to 2004 in the Nam Co basin of the Tibetan Plateau. *Chinese Science Bulletin*, 55, 1294–1303.

